Proceedings of the 2001 IEEE
International Conference on Robotics & Automation
Seoul, Korea · May 21-26, 2001

A Simulator to Analyze Creeping Locomotion of a Snake-like Robot

Shugen MA[1,3], Wen J. LI[2], Yuechao WANG[3]

[1]Dept. of Systems Engineering
Faculty of Eng., Ibaraki University
4-12-1 Nakanarusawa, Hitachi-Shi
Ibaraki-Ken, 316-8511 JAPAN
shugen@dse.ibaraki.ac.jp

[2]Dept. of Automation/Computer-Aided Eng.
The Chinese University of Hong Kong
MMW 425, Shatin, N. T., Hong Kong
P. R. CHINA
wen@acae.cuhk.edu.hk

[3] Robotics Laboratory, CAS
Shenyang Inst. of Automation
114 Nanta Str., Shenyang
110015 P. R. CHINA
ycwang@ms.sia.ac.cn

Abstract

Snakes perform many kinds of movement that are adaptable to the environment. Utilizing the snake (*its forms and motion*) as a model to develop a snake-like robot that emulates a snakes' function is important for generating a new type of locomotor and expanding the possible use of robots. In this study, we developed a simulator to simulate the creeping locomotion of a snake-like robot, in which the robot dynamics is modeled and its interaction with the environment is considered through Coulomb friction. This simulator makes possible to analyze the creeping locomotion with the normal-direction slip coupled to gliding along the tangential direction. Through the developed simulator, we investigated the snake-like robot creeping locomotion which is generated only by swinging each of the joints from side to side, and discussed the optimal creeping locomotion of the snake-like robot that is adaptable to a given environment.

1 Introduction

Snakes perform many kinds of movement that are adaptable to a given environment. Instead of being handicapped, the lack of limps, the considerable elongation of the body, and the particular mode of locomotion have allowed snakes to expand into diverse environments. One of the snakes' assets is their ability to immediately respond to a new environment by changing modes. This research aims to utilize the snake (*its forms and motion*) as a model to develop a snake-like robot to emulate the locomotive functions of a snake. Snakes are so diversified that they exhibit many examples of locomotive specializations, but in which one reptantion mode is always favored by a particular kind of snake. When these reptantions are broadly classified, there exist four gliding modes [1] [2]: 1) Serpentine movement, 2) Rectilinear movement, 3) Concertina movement, and 4) Side winding movement. However, the Serpentine movement (*Creeping locomotion*) is the movement to be seen typically in almost all kinds of snake, and is a gliding mode whose characteristic is that each part of the body makes similar tracks. In this study, we concentrate on the analysis of the serpentine movement.

Snake as a biological machine, in spite of its simplicity, performs well in terms of changing its highly redundant body to adapt to the environment. Several snake-like robots that emulate snakes' motion were developed [12]. The first serpentine robot was built by Hirose [3], who recently carried out the gliding experiments on ice to show that the creeping motion is same as the principle of skating [4]. How such mechanisms can locomote in a plane was studied in [3], [5], and [6]. The snake robot locomotion theory based on Geometric Mechanics was also discussed for the serpentine robot [7]. NEC developed a 3-dimensional motion robot for the purpose of search and rescue for survivors in collapsed buildings [10], and GMD built another 3-dimension motion robot by tendon-driven mechanism [11]. Beside the analysis of the serpentine motion, other movements were also analyzed [8] [9] [11]. The robots which were developed or theoretically analyzed for serpentine motion, were assumed to creep along a given curve path without any sliding in the direction normal to the body axis. The snake-like robots, however, are always slipping in the normal direction, adding to the glide along the tangential direction.

In this study, we developed a simulator to simulate the creeping locomotion of the snake-like robot, in which the robot dynamics is modeled and interaction with the environment is considered through Coulomb friction. This simulator makes possible to analyze the creeping locomotion with the normal-direction slip, adding to the glide along the tangential direction. Through the developed simulator, we investigate the snake-like robot creeping locomotion which is generated only by rolling each of the joints from side to side, and discuss the optimal creeping locomotion of the snake-like robot, which is adaptable to a given environment.

2 Simulator of a Snake-like Robot for Creeping Locomotion Analysis

The snake-like robot, shown in figure 1, is formed from serially-connected links. Each link is swung by electrical motor. The creeping locomotion of the snake-like robot is generated by swinging the joints from side to side to cause the forward (*or propelling*) force, which comes out from interaction of the robot with the environment through friction. In order to analyze the motion of the snake-like robot in the

0-7803-6475-9/01/$10.00© 2001 IEEE

case of considering the normal slip, the robot dynamics and friction with the environment must be modeled. In this section, we first model the robot and environment dynamics, and then develop a simulator for analyzing the creeping locomotion of the snake-like robot.

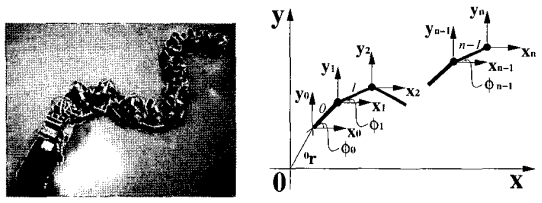

(a) Robot model (b) Coordinates

Fig. 1: Model of the snake-like robot and coordinates located on the robot

2.1 Motion Equations of the Robot

As shown in figure 1 (b), we locate each coordinates on the joints of the robot. The displacement of the joints and the displacement of the gravity center of the links, thus can be given by

$$ {}^{i+1}\boldsymbol{r} = {}^{0}\boldsymbol{r} + \sum_{j=0}^{i} \ell_j \begin{bmatrix} c_j \\ s_j \end{bmatrix}, \quad {}^{i}\boldsymbol{r}_G = {}^{i}\boldsymbol{r} + \ell_{Gi} \begin{bmatrix} c_i \\ s_i \end{bmatrix} \quad (1) $$

where ℓ_i is length of link i, ℓ_{Gi} is the distance of gravity center of link i from joint i, and $i = 0, 1, 2, \cdots, n-1$. Moreover, ${}^{n}\boldsymbol{r}$ is the displacement of head. The velocity and acceleration of the joints and those of the gravity center of the links can be derived through time-differentiation. For simplicity, we set $s_k = \sin(\phi_k)$ and $c_k = \cos(\phi_k)$ in the formulation.

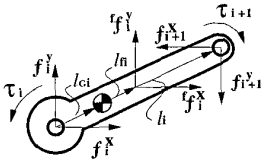

Fig. 2: Forces acted on the link

On the other hand, we model each link as that shown in figure 2. On the basis of the Newton-Euler equation, the robot dynamics can be derived and summarized as

$$ \mathbf{D}\boldsymbol{\tau} = {}^{f}\boldsymbol{\tau} + {}^{0}\boldsymbol{\tau} + \mathbf{M}_0 {}^{0}\ddot{\boldsymbol{r}} + \mathbf{M}\ddot{\boldsymbol{\phi}} \quad (2) $$

where

$$ \boldsymbol{\tau} = \begin{bmatrix} \tau_1 & \tau_2 & \cdots & \tau_{n-1} \end{bmatrix}^T \in \Re^{n-1} $$

$$ {}^{0}\ddot{\boldsymbol{r}} = \begin{bmatrix} {}^{0}\ddot{x} & {}^{0}\ddot{y} \end{bmatrix}^T \in \Re^2 $$

$$ \ddot{\boldsymbol{\phi}} = \begin{bmatrix} \ddot{\phi}_0 & \ddot{\phi}_1 & \cdots & \ddot{\phi}_{n-1} \end{bmatrix}^T \in \Re^n $$

$$ \mathbf{D} = \left\{ D_{(i,j)} \right\} \in \Re^{n \times (n-1)}, \quad D_{(i,j)} = \begin{cases} -1, & i = j \\ 1, & i = j+1 \\ 0, & \text{others} \end{cases} $$

$$ {}^{f}\boldsymbol{\tau} = \left\{ {}^{f}\tau_{(i)} \right\} \in \Re^n $$

$$ {}^{f}\tau_{(i)} = (\ell_i \sum_{k=i+1}^{n-1} {}^{f}f_k^x + \ell_{fi} {}^{f}f_i^x) s_i - (\ell_i \sum_{k=i+1}^{n-1} {}^{f}f_k^y + \ell_{fi} {}^{f}f_i^y) c_i $$

$$ {}^{0}\boldsymbol{\tau} = \left\{ {}^{0}\tau_{(i)} \right\} \in \Re^n $$

$$ {}^{0}\tau_{(i)} = \ell_i \sum_{k=i+1}^{n-1} (m_k \ell_{Gk} + \ell_k \sum_{j=k+1}^{n-1} m_j) \sin(\phi_k - \phi_i) \dot{\phi}_k^2 $$

$$ -(m_i \ell_{Gi} + \ell_i \sum_{j=i+1}^{n-1} m_j) \sum_{k=0}^{i-1} \ell_k \sin(\phi_k - \phi_i) \dot{\phi}_k^2 $$

$$ \mathbf{M}_0 = \left\{ \boldsymbol{M}_{0(i)}^T \right\} \in \Re^{n \times 2} $$

$$ \boldsymbol{M}_{0(i)} = (m_i \ell_{Gi} + \ell_i \sum_{k=i+1}^{n-1} m_k) \begin{bmatrix} -s_i & c_i \end{bmatrix}^T \in \Re^2 $$

$$ \mathbf{M} = \left\{ M_{(i,j)} \right\} \in \Re^{n \times n} $$

$$ M_{(i,j)} = \begin{cases} \ell_i (m_j \ell_{Gj} + \ell_j \sum_{k=j+1}^{n-1} m_k) \cos(\phi_j - \phi_i), & j < i \\ m_i \ell_{Gi}^2 + I_i + \ell_i^2 \sum_{k=i+1}^{n-1} m_k, & j = i \\ (m_i \ell_{Gi} + \ell_i \sum_{k=i+1}^{n-1} m_k) \ell_j \cos(\phi_j - \phi_i), & j > i \end{cases} $$

Therein, τ_i is the torque at joint i, m_i and I_i are the mass and the moment inertia of link i, and $i = 0, 1, 2, \cdots, n-1$. Note that at the tail and the head there are no actuators, thus $\tau_0 = 0$ and $\tau_n = 0$.

Moreover, since the snake-like robot has no fixed base, the forces must satisfy

$$ {}^{f}\boldsymbol{f} + {}^{0}\boldsymbol{f} + \mathbf{m}_0 {}^{0}\ddot{\boldsymbol{r}} + \mathbf{m}\ddot{\boldsymbol{\phi}} = 0 \quad (3) $$

where

$$ {}^{f}\boldsymbol{f} = \begin{bmatrix} \sum_{k=0}^{n-1} {}^{f}f_k^x & \sum_{k=0}^{n-1} {}^{f}f_k^y \end{bmatrix}^T \in \Re^2 $$

$$ {}^{0}\boldsymbol{f} = \begin{bmatrix} -\sum_{k=0}^{n-1} (m_k \ell_{Gk} + \ell_k \sum_{j=k+1}^{n-1} m_j) c_k \dot{\phi}_k^2 \\ -\sum_{k=0}^{n-1} (m_k \ell_{Gk} + \ell_k \sum_{j=k+1}^{n-1} m_j) s_k \dot{\phi}_k^2 \end{bmatrix} \in \Re^2 $$

$$ \mathbf{m}_0 = \sum_{k=0}^{n-1} m_k \begin{bmatrix} 1 & 0 \\ 0 & 1 \end{bmatrix} \in \Re^{2 \times 2} $$

$$\mathbf{m} = \left\{ \boldsymbol{m}_{(j)} \right\} \in \Re^{2\times n}$$

$$\boldsymbol{m}_{(j)} = \begin{bmatrix} -(m_j \ell_{Gj} + \ell_j \sum_{k=j+1}^{n-1} m_k) s_j \\ (m_j \ell_{Gj} + \ell_j \sum_{k=j+1}^{n-1} m_k) c_j \end{bmatrix} \in \Re^2$$

2.2 Environment Dynamics

We utilize the edge or the wheel to generate the different friction between the tangential and normal directions. The Coulomb friction was used to define the environment dynamics, and given by

$$ {}^f f_i^e = \begin{cases} -{}^f f_s^e \frac{\delta^i r^e}{l_s^e}, & \delta^i r^e \le l_s^e \\ -\mu_e m_i g \times \mathrm{sign}(\delta^i r^e), & \delta^i r^e > l_s^e \end{cases} \quad (4)$$

where $e = t, n$. μ_t and μ_n express the friction coefficients in tangential direction and normal direction, while ${}^f f_s^t$ and ${}^f f_s^n$ are the maximum static friction forces in tangential and normal directions. l_s is the maximum value of the displacement $\delta^i r$ at the friction point for changing to dynamic friction from static friction.

The friction forces along the $x-$ and $y-$ axes can be obtained, if we define the angle of tangential force to $x-$axis as ψ (*it is ϕ if the edge is parallel to or along the link axis*), by

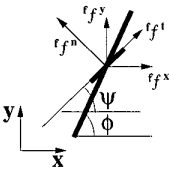

$$ {}^f f_i^x = {}^f f_i^t \cos\psi_i - {}^f f_i^n \sin\psi_i \quad (5)$$

$$ {}^f f_i^y = {}^f f_i^t \sin\psi_i + {}^f f_i^n \cos\psi_i \quad (6)$$

2.3 Body Shape

For convenience, we use the Serpenoid curve as the basic body shape of the snake-like robot, while it creeps on the plane. The Serpenoid curve is given by the curvature function

$$\kappa(s_p) = -\frac{2K_n \pi \alpha_0}{L} \sin(\frac{2K_n \pi}{L} s_p) \quad (7)$$

where K_n gives number of the $S-$shape, α_0 is the initial winding angle, $L(= \sum_{k=0}^{n-1} \ell_k)$ is the whole length of robot body, and s_p is the body length along the body curve, respectively.

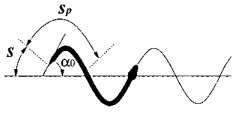

We assume that the snake-like robot holds its shape on the Serpenoid curve and the body shape changes with respect to the change of the Serpenoid curve while moving in the plane. In this case, the joint variables in relative value are derived from integration of the curvature function given in equation (7). With the assumption that $\ell_i = \ell$ and $L = n\ell$ we have

$$\theta_i = \int_{s+s_{p_{i-1}}+\frac{1}{2}\ell}^{s+s_{p_i}+\frac{1}{2}\ell} \kappa(u)du = \int_{s+(i-1)\ell+\frac{1}{2}\ell}^{s+i\ell+\frac{1}{2}\ell} \kappa(u)du$$
$$= -2\alpha_0 \sin(\frac{K_n\pi}{n}) \sin(\frac{2K_n\pi}{L} s + \frac{2K_n\pi}{n} i) \quad (8)$$

where $i = 1, 2, \cdots, n-1$ (*n: Number of joints*), s is the virtual displacement of the tail along the Serpenoid curve path that determines the changing frequency of the body curve. The joint velocities and accelerations can be derived by differentiating equation (8) with respect to time.

2.4 Shape to Motion: $\boldsymbol{\theta} \Longrightarrow {}^0\boldsymbol{r}, \phi_0, \boldsymbol{\tau}$

How the snake-like robot moves by changing its body shape is discussed below. Specifically giving the joint variables $\boldsymbol{\theta}(t)$, $\dot{\boldsymbol{\theta}}(t)$, and $\ddot{\boldsymbol{\theta}}(t)$, the whole robot motion needs to be derived. From the relation of the absolute value of joint angles to their relative value, $\phi_i = \phi_{i-1} + \theta_i$, we have,

$$\boldsymbol{\phi} = \mathbf{E}\boldsymbol{\theta} + \boldsymbol{e}\phi_0 \quad (9)$$

where $\boldsymbol{e} = \begin{bmatrix} 1 & \cdots & 1 \end{bmatrix}^T \in \Re^n$, and $\mathbf{E} = \left\{ E_{(i,j)} \right\} \in \Re^{n\times(n-1)}$, $E_{(i,j)} = \begin{cases} 1, & i > j \ \ \& \ \ i > 1 \\ 0, & \text{others} \end{cases}$.

Solving equation (3) and substituting equation (9) into it, we obtain

$$ {}^0\ddot{\boldsymbol{r}} = -\mathbf{m}_0^{-1}\mathbf{m}\ddot{\boldsymbol{\phi}} - \mathbf{m}_0^{-1}({}^f\boldsymbol{f} + {}^0\boldsymbol{f})$$
$$= -\mathbf{m}_0^{-1}\mathbf{m}(\mathbf{E}\ddot{\boldsymbol{\theta}} + \boldsymbol{e}\ddot{\phi}_0) - \mathbf{m}_0^{-1}({}^f\boldsymbol{f} + {}^0\boldsymbol{f}) \quad (10)$$

Substituting equation (10) into equation (2), we have

$$\mathbf{D}\boldsymbol{\tau} + (\mathbf{M}_0\mathbf{m}_0^{-1}\mathbf{m} - \mathbf{M})\boldsymbol{e}\ddot{\phi}_0 = (\mathbf{M} - \mathbf{M}_0\mathbf{m}_0^{-1}\mathbf{m})\mathbf{E}\ddot{\boldsymbol{\theta}}$$
$$+ {}^f\boldsymbol{\tau} + {}^0\boldsymbol{\tau} - \mathbf{M}_0\mathbf{m}_0^{-1}({}^f\boldsymbol{f} + {}^0\boldsymbol{f}) \quad (11)$$

Equation (11) is a $n-$dimensional linear equation of n unknown variables $\boldsymbol{\tau}$ ($\in \Re^{n-1}$) and $\ddot{\phi}_0$ ($\in \Re$). Solving equation (11), we thus can obtain the joint torques $\boldsymbol{\tau}$ and the first link rotation acceleration $\ddot{\phi}_0$. Substituting these values into equation (10), we can have the first joint moving acceleration ${}^0\ddot{\boldsymbol{r}}$. The first link rotation velocity $\dot{\phi}_0$ and its angle ϕ_0, the first link moving velocity ${}^0\dot{\boldsymbol{r}}$ and its moving distance ${}^0\boldsymbol{r}$, are obtained through integration. Thus, the robot motion is derived in the case of body-shape changing. The necessary joint torques to generate the robot motion are obtained at the same time.

2.5 Torque to Motion: $\boldsymbol{\tau} \Longrightarrow {}^0\boldsymbol{r}, \phi$

How the snake-like robot moves given torque input to each joint is discussed here. Specifically giving the joint torques $\boldsymbol{\tau}(t)$, the whole robot motion is derived. Substituting equation (10) into equation (2), we have

$$(\mathbf{M} - \mathbf{M}_0\mathbf{m}_0^{-1}\mathbf{m})\ddot{\boldsymbol{\phi}} = \mathbf{D}\boldsymbol{\tau}$$
$$- {}^f\boldsymbol{\tau} - {}^0\boldsymbol{\tau} + \mathbf{M}_0\mathbf{m}_0^{-1}({}^f\boldsymbol{f} + {}^0\boldsymbol{f}) \quad (12)$$

Equation (12) is also a $n-$dimensional linear equation of n unknown variables $\ddot{\boldsymbol{\phi}}$ ($\in \Re^n$). Solving this equation, we thus can obtain the link rotation acceleration $\ddot{\boldsymbol{\phi}}$. Substituting these values into equation (10), the first joint moving acceleration ${}^0\ddot{\boldsymbol{r}}$ can be obtained. Same as above, the link rotation velocities $\dot{\boldsymbol{\phi}}$, the joint rotation angles $\boldsymbol{\phi}$, the first link moving velocity ${}^0\dot{\boldsymbol{r}}$ and its moving distance ${}^0\boldsymbol{r}$, are obtained through integration. Thus, the robot motion is derived in the case of torque input to each joint.

2.6 Simulator for Creeping Locomotion

Based on the above formulation, the simulator shown in figures 3 was developed to simulate the creeping locomotion of the snake-like robot, with consideration of robot dynamics and interaction with the environment. The input of the simulator is joint torques and its output is the whole robot motion. This simulator makes possible to analyze the creeping locomotion of snake-like robot with the normal-direction slip, coupling to the glide along the tangential direction.

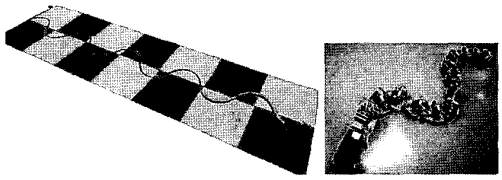

Fig. 3: Simulator of the snake-like robot

3 Optimal Body-shape for Creeping Locomotion

Snakes change their body shape to adapt to the environment change. To find the exact optimal body shape is not an easy task. In this study, we assume that the snake-like robot is constrained to move in a Serpenoid curve, and derive the quasi-optimal body shape among the Serpenoid curves.

The physical parameters (*number of links n and link length ℓ*) are determined from the Robot model, the motion parameters (*virtual motion of tail along the Serpenoid curve path or change of the body shape, $s, \dot{s}, \ddot{s}$*) are given by the user, and only the parameters (*number of $S-$shape K_n and initial winding angle α_0*) are variable. As known from equations in section 2, while s, $\dot{s}$, and $\ddot{s}$ are given, the motion distance, the joint torques, and the slip in the direction normal to the body depend upon the number of $S-$shape K_n and the initial winding angle α_0, and of course, also depend upon the environment change through the friction force ${}^f\boldsymbol{f}$.

We can thus define the locomotive efficiency as

$$J = \frac{S}{\frac{1}{T}\int_0^T \sum_1^{n-1} \tau_i^2 dt * \frac{1}{T}\int_0^T \sum_0^n |\delta^i r^n| dt} \qquad (13)$$

where S is the total motion distance ($\rightarrow$ *maximization*), $\frac{1}{T}\int_0^T \sum_0^n |\delta^i r^n| dt$ is average of the normal-direction slipping distance ($\rightarrow$ *minimization*), and $\frac{1}{T}\int_0^T \sum_1^{n-1} \tau_i^2 dt$ is average of the square-sum of torques ($\rightarrow$ *minimization*), respectively. The criterion given in equation (13) is to minimize the joint torques together with the normal direction slip, and to maximize motion distance. As seen from the computer simulation (*in section 4*), changing the number of $S-$shape K_n does not affect much the locomotive efficiency if $K_n \geq 2$. If we give the number of $S-$shape K_n, the problem of obtaining the optimal body posture is thus changed to derive the optimal winding angle α_0 that maximizes the locomotive efficiency J. This problem can be simply solved by the Golden Section Search algorithm.

4 Computer Simulations

Using the developed simulator, we investigate here the snake-like robot creeping locomotion which is generated only by swinging each of the joints from side to side. Three experimental tests of the computer simulation were performed and their results are introduced in this section. Table I shows the parameters used in the experiments. In simulation one, the initial winding angle $\alpha_0 = 60^\circ$ [deg] and the number of S-shape $K_n = 1$ were used.

Table I: Parameters used in experimental tests

Number of joints n	20
Length of link ℓ	0.08 [m]
Mass of link m	0.5 [kg]
Inertia of link I	0.016 [kgm^2]
G.C. position of link ℓ_G	0.02 [m]
Contact point ℓ_f	0.04 [m]

Simulation One: Shape to Motion

The body shape is changed with respect to s ($\dot{s}$, $\ddot{s}$), and the relative values of joint variables are calculated through equations (8). The acceleration $\ddot{s}$ is given by

$$\ddot{s} = \begin{cases} a, & 0 \leq t < T/10 \\ 0, & T/10 \leq t < 9T/10 \\ -a, & 9T/10 \leq t < T \end{cases}$$

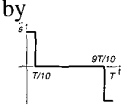

where T is the motion time, and a is the acceleration input. $T = 8.0$ [s] and $a = 1$ [m/s^2] were used in the simulation.

Two different environments were considered. Case one is $\mu_t = 0.001$, $\mu_n = 0.5$, $l_s^n = 0.00001$ [m], ${}^f f_s^n = 5$ [N], and $l_s^t = 0.0$ [m], ${}^f f_s^t = 0$ [N]; Case two is $\mu_t = 0.2$, $\mu_n = 0.5$, $l_s^n = 0.00001$ [m], ${}^f f_s^n = 4$ [N], and $l_s^t = 0.0$ [m], ${}^f f_s^t = 0$ [N]. The robot motion is shown in figure 4. As seen, larger the tangential friction force and/or smaller the normal friction force are, more the normal-direction slip generates and lower the locomotive efficiency (*smaller mo-*

tion distance). Figure 5 shows the example of the corresponding torques of joints 1, 5, 10, 15, and 19 to generate the robot motion shown in figure 4. They are obtained by solving equation (11) at the same time of deriving the robot motion. It is known that the input torques at the joints are near-cyclicly changed and their values are affected by the environment.

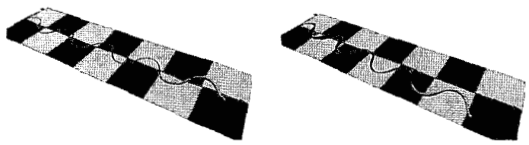

(a) Case One (b) Case Two

Fig. 4: Creeping locomotion of the snake-like robot on two different environments

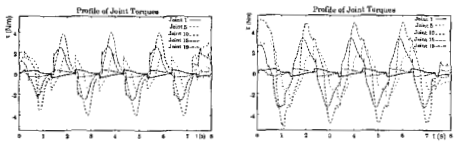

(a) Case One (b) Case Two

Fig. 5: Example of corresponding joint torques on different environments (Joints $1, 5, 10, 15, \&19$)

Simulation Two: Torque to Motion

The joint torque input is simply given by

$$\tau_i = \tau_{max} \sin(2\pi \frac{i}{n} + t) \qquad (i = 1, 2, \cdots, n-1) \quad (14)$$

where $\tau_{max} = 0.8$ [Nm] was used in the simulation. The robot is assumed to move on the environment where $\mu_t = 0.001$, $\mu_n = 0.9$, $l_s^n = 0.00001$ [m], ${}^f f_s^n = 5$ [N], and $l_s^t = 0.0$ [m], ${}^f f_s^t = 0$ [N]. Figure 6 shows the obtained robot motion. It is known that even though only giving the torque input by a simple function, the snake-like robot does creep and go forward.

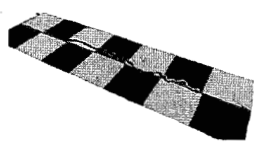

Fig. 6: Creeping movement of the snake-like robot in the case of giving a simple torque input

Simulation Three: Quasi-optimal Body Shape

In the case that we assume that the snake-like robot is constrained onto the Serpenoid curve, the quasi-optimal body shape from the Serpenoid curves is derived here. It is known that while the virtual motion of tail s is given, the motion distance, the joint torques, and the slip distance in the direction normal to the body depend upon the number of $S-$shape K_n and the initial winding angle α_0, also depend upon the environment change.

First, we plot the average of the square-sum of torques, the average of the normal-direction slipping distance, and the total motion distance, corresponding to the number of $S-$shape K_n and the environment change ($\mu_n = 0.8$, $\mu_t = 0.0 \sim 0.8$). Therein, the initial winding angle α_0 is fixed at $\alpha_0 = 60^0$. The results are shown in figure 7. From the results, we know that change of the number of $S-$shape K_n does not affect much the performance when $K_n \geq 2$. For possible forward motion, almost the same normal-direction slipping distance and the same total motion distance were generated, and the joint torques show little difference for $K_n \geq 2$. As a result, we conclude that the number of $S-$shape K_n does not give large influence on the performance and can be given by the user.

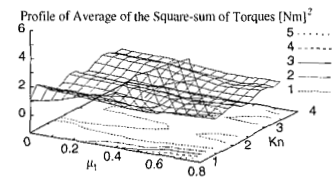

(a) Average of the square-sum of torques

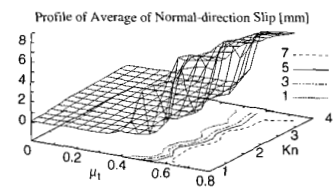

(b) Average of the normal-direction slipping distance

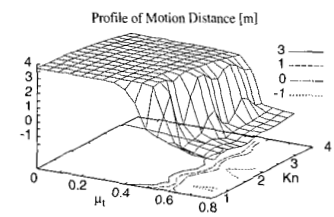

(c) Total motion distance S

Fig. 7: Performance corresponding to number of $S-$**shape** K_n **and environment change, while** $\alpha_0 = 60^0$

Then, we consider the average of the square-sum of torques, the average of the normal-direction slipping distance, and the total motion distance, corresponding to the initial winding angle α_0 and the environment change ($\mu_n = 0.8$, $\mu_t = 0.0 \sim 0.8$), while the number of $S-$shape K_n equals 1, 2, and 3. They are shown in figure 8. From the results, we also know that the number of $S-$shape K_n does not give large influence on the performance, but the initial winding angle α_0 largely affect the performance, when

$K_n \geq 2$. From the above results, it is known that, 1) the

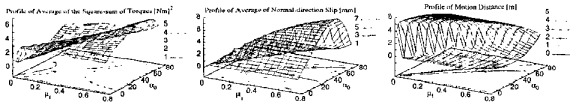

(a) $K_n = 1$

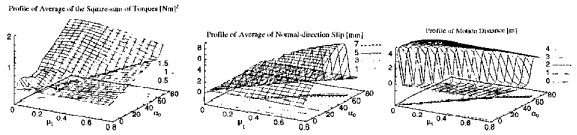

(b) $K_n = 2$

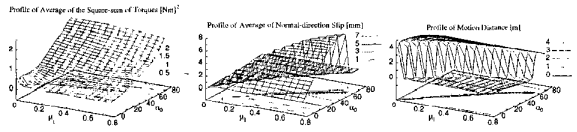

(c) $K_n = 3$

Fig. 8: Performance corresponding to initial winding angle α_0, while the number of $S-$shape K_n equals 1, 2, and 3

number of $S-$shape K_n does not give large influence on the performance, and it can be given by the user, 2) the initial winding angle α_0 largely affect the performance, thus should be changed in order to adapt to environment change, 3) the optimal body shape adapted to the environment exists which optimizes the locomotive efficiency.

Next, we derive the quasi-optimal body shape that maximizes the locomotive efficiency given by equation (13). On an environment of $\mu_n = 0.8$, $l_s^n = 0.0$ $[m]$, ${}^f f_s^n = 5$ $[N]$, and $\mu_t = 0.0 \sim 0.3$, $l_s^t = 0.0$ $[m]$, ${}^f f_s^t = 0$ $[N]$, the obtained optimal winding angle α_0 is shown in figure 9 (a) and the corresponding performance criterion is in figure 9 (b). From the results, it is shown that the smaller initial winding angle α_0 needs to adapt to the environment change for the case of the larger number of $S-$shape K_n. When $K_n \geq 2$, the optimal initial winding angle α_0 and the corresponding performance criterion have no big change while the number of $S-$shape K_n changes. In addition, we also know that the optimal initial winding angle α_0 exists to adapt to the environment change: larger the tangential friction force and/or smaller the normal friction force are, the larger initial winding angle α_0 optimizes the locomotive efficiency, and vice versa.

5 Conclusions

In this study, we developed a simulator to simulate the creeping locomotion of the snake-like robot, in which the robot dynamics is modeled and the interaction with the environment is considered through Coulomb friction. This simulator makes possible to analyze the creeping locomotion with the normal-direction slip, coupling to the glide

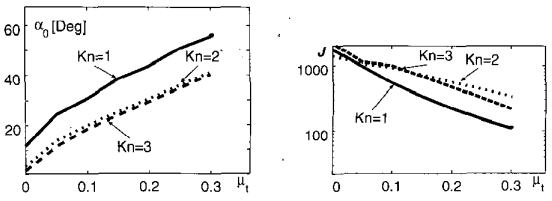

(a) Optimal Angle α_0 (b) Corresponding Criterion

Fig. 9: Optimal winding angle α_0 and corresponding performance criterion, while $K_n = 1$, $K_n = 2$, and $K_n = 3$

along the tangential direction. Through the developed simulator, we investigated the snake-like robot creeping locomotion which is generated only by swinging each of the joints from side to side, and discussed the optimal creeping locomotion of the snake-like robot that is adaptable to the environment. The best function for joint torque input to get optimal creeping locomotion and the optimal body shape to adapt to the environment will be discussed in future studies.

At last, we acknowledged that this research is partially supported by the Ministry of Education, Science, Sports, and Culture of Japan, Grants-in-Aid (No. 10751081), and Hayao Nakayama Foundation for Science & Technology and Culture.

References

[1] J. Gray, *Animal Locomotion*, pp.166/193, Norton, 1968

[2] R. M. Alexander, *Exploring Biomechanics — Animals in Motion*, W. H. Freeman and Company, 1992

[3] S. Hirose, *Biologically Inspired Robot — Snake-like locomotors and manipulators*, Oxford University Press, 1993

[4] G. Endo, K. Togawa, and S. Hirose, *Study on Self-constrained and Terrain Adaptive Active Cord Mechanism*, in Proc. Int. Conf. on Intelligent Robots and Systems (IROS'99), pp.1399/1405, 1999

[5] S. Ma, *Analysis of Snake Movement Forms for Realization of Snake-like Robots*, in Proc. 1999 IEEE Int. Conf. on Robotics and Automation (ICRA'99), pp.3007/3013, 1999

[6] A. Naito and S. Ma, *Analysis of Creeping Locomotion of Snake-like Robots*, in Proc. 3rd Asian Conf. on Robotics and its Application (3rd ACRA), pp.393/398, 1997

[7] J. Ostrowski and J. Burdick, *Geometric Perspectives in the Mechanics and Control of Robotic Locomotion*, in Proc. 7th Int. Symp. Robotics Research, pp.487/504, 1995.

[8] G.S. Chirikjian and J.W. Burdick, *The Kinematics of Hyper-Redundant Robotic Locomotion*, IEEE Trans. on Robotics and Automation, **11**-6, pp.781/793, 1995

[9] J. Burdick, J. Radford, and G.S. Chirikjian, *A Sidewinding Locomotion Gait for Hyper-Redundant Robots*, Int. J. Advanced Robotics, **9**-3, pp.195/216, 1995

[10] O. Takanashi, K. Aoki, and S.Yashima, *A Gait Control for the Hyper-redundant Robot O-RO-CHI*, in Proc. 8th JSME Annual Conference on Robotics and Mechatronics, 1996, pp.78–80 (in Japanese)

[11] R. Worst, and R. Linnemann, *Construction and Operation of a Snake-like Robot*, in Proc. IEEE International Joint Symposia on Intelligence and Systems, 1996

[12] http://borneo.gmd.de/~worst/snake-collection.html